Thermodynamic Analysis of Decomposition of Thiourea and Thiourea Oxides

Shun Wang,[†,‡] Qingyu Gao,*[,†] and Jichang Wang*[,§]

College of Chemical Engineering, China University of Mining and Technology, Xuzhou, Jiangsu, China, 221008, Department of Chemistry and Material Science, Wenzhou Normal College, Wenzhou, China, 325027, and Department of Chemistry and Biochemistry, University of Windsor, Ontario, Canada N9B 3P4

Received: March 30, 2005; In Final Form: June 29, 2005

Thiourea has exhibited extremely rich dynamical behavior when being oxidized either through a chemical approach or via an electrochemical method. In this study, thermodynamic properties of thiourea and its oxides are investigated by measuring their thermogravimetry (TG), differential thermogravimetry (DTG), and differential scanning calorimetry (DSC) simultaneously. Online FT-IR measurements show that products of the thermal decomposition vary significantly with the reaction temperature. In addition to the determination of their apparent activation energy (E), preexponential factor (A), and entropy ($\Delta S^{\ddagger}$), enthalpy ($\Delta H^{\ddagger}$), and Gibbs energy ($\Delta G^{\ddagger}$) of thermal decomposition, our investigation further illustrates that the decomposition kinetics of thiourea and thiourea oxides follows the Johnson−Mehl−Avrami Equation, $f(\alpha) = n(1 - \alpha)[-\ln(1 - \alpha)]^{1-1/n}$ and $G(\alpha) = [-\ln(1 - \alpha)]^{1/n}$ with n equal to 2, 3.43, and 3, respectively.

1. Introduction

Thiourea (TU) and its oxides are important reagents in various industrial productions.[1−7] For example, thiourea has been used widely as an additive to improve coating quality and to inhibit corrosion.[1,2] It has also been used as an efficient reactant to synthesize heterocycles and to extract precious metals.[3,4] Thiourea dioxide, aminoiminomethanesulfinic acid (AIMSA), is commonly employed as a powerful bleaching reagent in the textile industry[5] and as an effective initiator for various polymerizations.[6,7] Thiourea trioxide, aminoiminomethanesulfonic acid (AIMSOA), however, is found to be a convenient guanidylating agent, which is known to present as a subunit in the amino acid arginine, the pyrimidine base of DNA, and many other biologically significant molecules.[8−11]

In addition to the practical applications mentioned above, thiourea and thiourea oxides are also valuable reactants in fundamental scientific researches, especially in the study of nonlinear reaction dynamics.[12−15] The oxidation of thiourea has displayed various fascinating nonlinear dynamical behaviors such as oligooscillations, autocatalysis in a closed system, mixed-mode oscillations, bistability, birhythmicity, quasiperiodicity and chaos in a continuously flow stirred tank reactor (CSTR), and travelling waves in a reaction−diffusion medium.[16−21] Only a few chemical systems are known to be capable of exhibiting such rich dynamics. Consequently, studies of the kinetics and mechanisms of the oxidation of thiourea and thiourea derivatives have attracted a great deal of attention in the past two decades, in which various oxidants such as iodate, bromate, chorite, chlorine dioxide, ferrate (VI), hydroxyl radicals, and peracetic acid have been characterized.[22−29] These earlier investigations led to a general conclusion that the oxidation of thiourea goes through S-oxygenation to form sulfenyl, then sulfinic and sulfonic acids, and finally sulfate ions. Yet, whether these rich nonlinear phenomena observed in thiourea oxidations arise from sulfur chemistry or from oxidants remains to be understood.[29,30] In particular, both simple and complex oscillations have been observed when thiourea was oxidized through an electrochemical approach.[31] Apart from scientific interests, knowing the oxidation kinetics of thiourea and thiourea oxides may also be critical in the understanding of the physiological effects of sulfur-containing species. In recent studies, Simoyi and his group conducted a series of experiments on the decomposition of thiourea dioxide in alkaline solution and their study suggests that the reactive oxygen species, superoxide, peroxide, and hydroxyl radicals that result from the cleavage of the C−S bond to give the sulfoxylate ion are responsible for the inherent toxicities of thiourea.[32]

To shed light on the oxidation kinetics of thiourea and its impacts on physiological and environmental aspects, in this study we characterized the thermal stabilities of thiourea and its oxides. It is motivated by the fact that although it is well known that violent oxidations or combustion of thiourea and thiourea oxides may result in the production of poisonous gases such as SO_2 and SO_3,[33] surprisingly little is known about their thermal decomposition kinetics. In the following, we investigate the pyrolysis of thiourea, AIMSA, and AIMSOA under nonisothermal conditions by a simultaneous TG/DTG/DSC-FT-IR method. Our study leads to the establishment of three kinetic equations to account for their decompositions.

2. Experimental Procedure

Reagent grade $SC(NH_2)_2$ was recrystallized twice with hot water that had been distilled and then purified through a Milli-Q system (18.2 MΩ). AIMSA (Aldrich) was used without further purification. AIMSOA was prepared according to literature and was identified by IR spectra measured with a Nicolet Avatar 360 FT-IR spectrometer.[10] The measured characteristic absorption wavenumbers of AIMSOA are 1220 cm^{-1} and 1050 cm^{-1}, which are in good agreement with theoretical values.[34] The

* Corresponding authors. E-mail: gaoqy@cumt.edu.cn; fax: 86-516-3995758. E-mail: jwang@uwindsor.ca; fax: 1-519-973-7098.
[†] China University of Mining and Technology.
[‡] Wenzhou Normal College.
[§] University of Windsor.

10.1021/jp051620v CCC: $30.25
Published on Web 08/20/2005

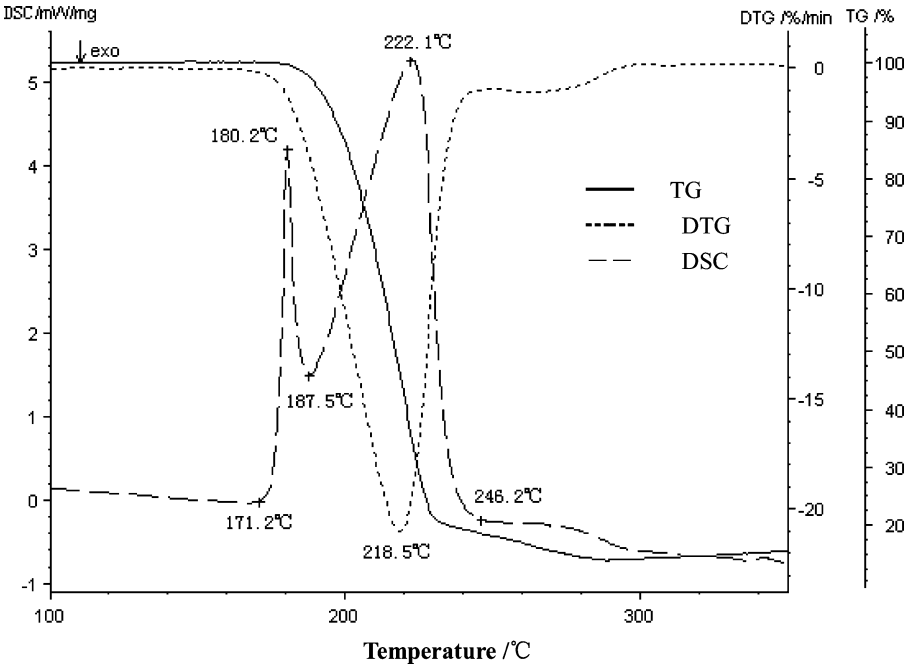

Figure 1. TG/DTG/DSC curves of the thermal decomposition of thiourea. The flow rate of nitrogen is 30.0 mL min^{-1}. The heating rate equals 8.0 °C min^{-1}, and the initial amount of thiourea is 6.40 mg.

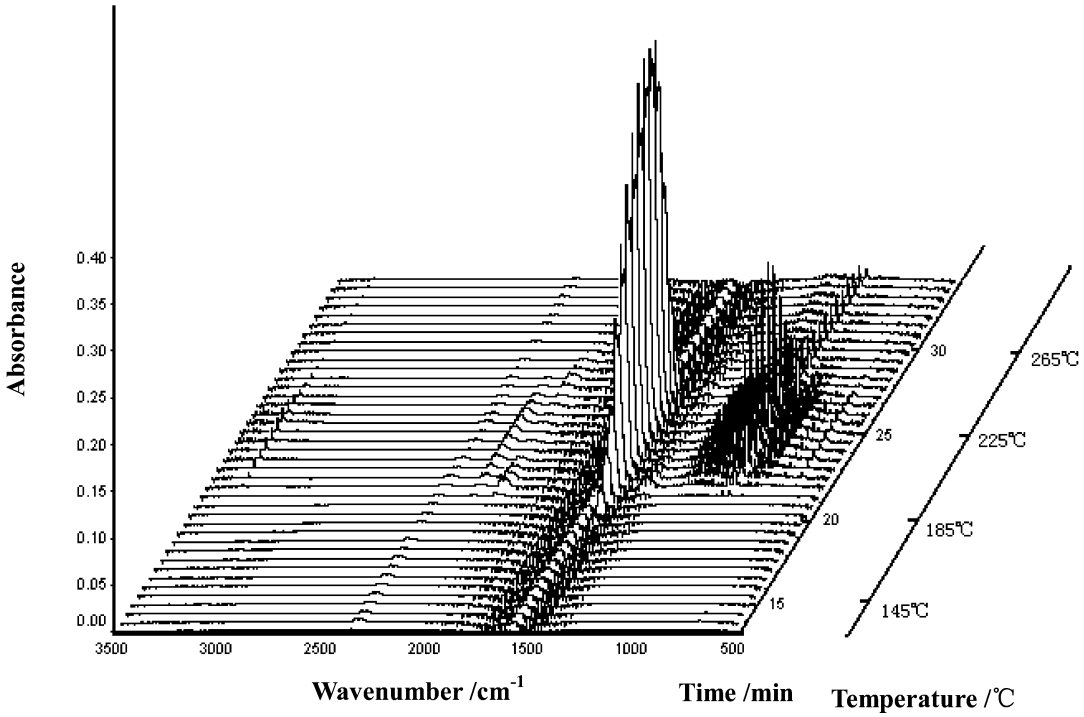

Figure 2. Online FT-IR spectra of the off-gases of the pyrolysis of thiourea. All of the reaction conditions are the same as those in Figure 1.

simultaneous TG/DTG/DSC measurements were carried out with a Netzsch STA 409C thermoanalyzer under nitrogen atmosphere. Throughout this study, the flow of nitrogen gas was fixed at 30.0 mL min^{-1}. The heating rate has been studied at 2.0, 5.0, 8.0, 12.0, and 15.0 °C min^{-1}, respectively. Samples of 3.0−9.0 mg were placed in a Al_2O_3 crucible, and the gas products of the thermal decomposition were analyzed online with a Nicolet Avatar 470 FT-IR spectrometer.

3. Experimental Results

Figure 1 presents the typical TG, DTG, and DSC curves of thiourea decomposition conducted at a heating rate of 8.0 °C min^{-1}. The DSC curve shows that there are two strongly overlapping endothermic processes in which the first endothermic process spans the temperature range between 171.2 and 187.5 °C with the maximum at 180.2 °C. As is indicated by the TG curve, during the first endothermic process there is nearly no mass loss. Therefore, the first endothermic process is dominated by the melting of thiourea.[35] Notably, in our experiments the initial point, T_0, at which the DSC curve deviates from the baseline is lower than the melting temperature of thiourea, which is reported to be around 175.05 °C and 179.05 °C.[36,37] In addition, the calculated reaction enthalpies yield an average value of 6.8 kJ·mol^{-1}, which is also less than 12.6

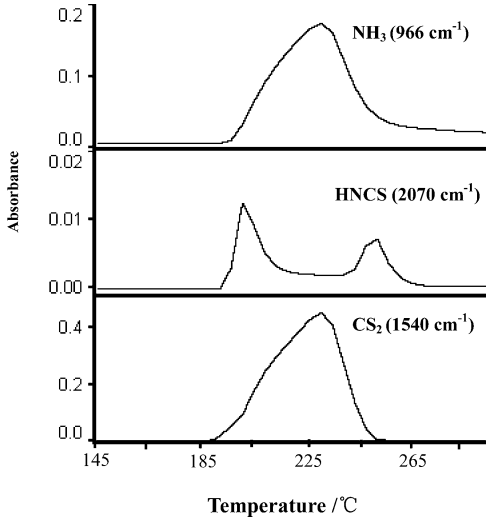

Figure 3. The absorbance vs temperature curves showing variations of concentrations of the thermal decomposition products as a function of temperature. The reaction conditions are listed in Figure 1.

kJ·mol^{-1} reported by other groups.[36] Because we had always used freshly prepared thiourea, the decomposition of thiourea (i.e., aging) is unlikely responsible for the above abnormal behavior. Isomerization of thiourea has been proposed earlier by Waddell in the study of the conversion of thiourea into thiocyanate. The production of $NH_4SCN(s)$, which has a lower melting temperature around 149.0 °C, would consequently reduce T_0 of the DSC curve. Thus, the isomeric reaction (R1) is suggested to take place within the temperature range between 171.2 and 187.5 °C.

$$SC(NH_2)_2(s) + \text{Heat} = NH_4SCN(s) \qquad (R1)$$

In contrast to the first endothermic process, the second endothermic process (between 187.5 and 246.2 °C with the peak temperature at 222.1 °C) governs more than 80% of the total weight loss. As is illustrated by the real time FT-IR spectra of the off-gases (see Figure 2), there are three major species in the thermal decomposition products, namely, carbon disulfide (CS_2) with absorption peaks at 1540 and 2171 cm^{-1}, isothiocyanic acid (HNCS) with absorption peaks at 2070 and 2041 cm^{-1}, and ammonia (NH_3) with absorption peaks at 3331, 1635, 966, and 925 cm^{-1}.[38,39] Figure 3 presents the corresponding evolution curves of the three reagents as a function of temperature, which clearly shows that the thermal decomposition of thiourea begins at 187.5 °C. As is shown by the DTG curve in Figure 1, the decomposition rate of thiourea increases rapidly with temperature and reaches the maximum at 218.5 °C. The production of CS_2, HNCS, and NH_3 are presumably dominated by the following two steps:

$$2SC(NH_2)_2(s) \rightarrow CS_2(g) + H_2NCN(g) + 2NH_3(g) \qquad (R2)$$

$$NH_4SCN(s) \rightarrow NH_3(g) + HNCS(g) \qquad (R3)$$

According to reaction R2, cyanamide (H_2NCN), which has a characteristic absorption peak at 2284 cm^{-1}, shall also appear in the IR spectra; yet no such a peak was seen in our experiments. An existing study suggested that $H_2NCN(g)$ may undergo a spontaneous polymerization reaction to produce melamine.[40] As a result, the escape of H_2NCN is retarded.

Figure 3 shows that despite the fact that the decomposition rate of thiourea reaches the maximum at T = 218.5 °C, concentrations of NH_3 and CS_2 will not reach their maximum until T = 228.6 °C. Meanwhile, the concentration of HNCS evolves through two extremes at 198.8 and 251.1 °C, respectively. To account for the dip in HNCS concentration, the following three reactions (R4−R6) have been proposed to occur around T = 220.0 °C.

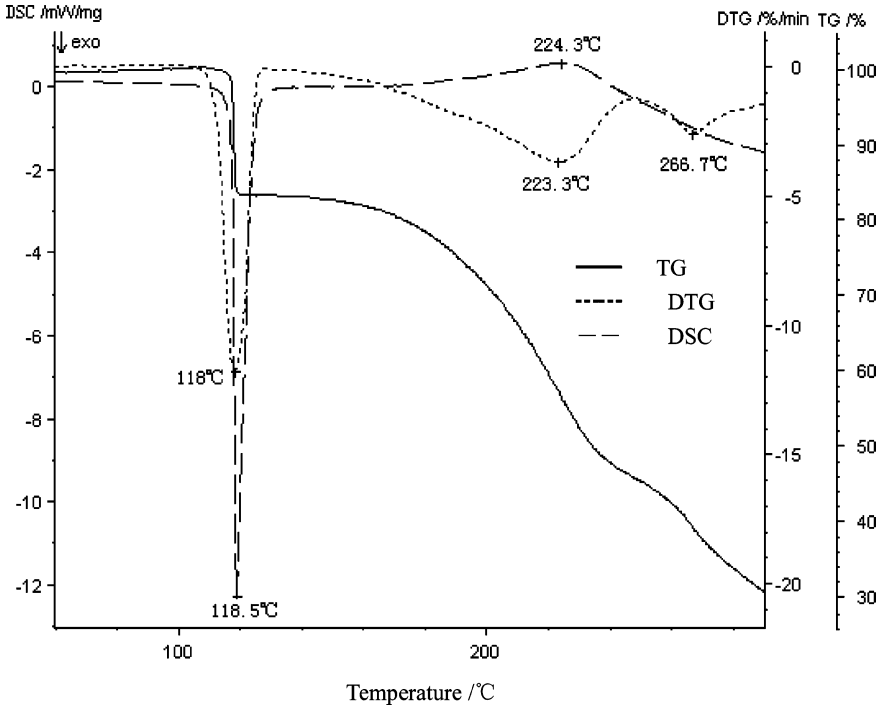

Figure 4. Simultaneous TG/DTG/DSC curves of the pyrolysis of thiourea dioxide. The flow of nitrogen equals 30.0 mL min^{-1}. The heating rate equals 5.0 °C min^{-1}, and the initial mass of thiourea dioxide is 8.10 mg.

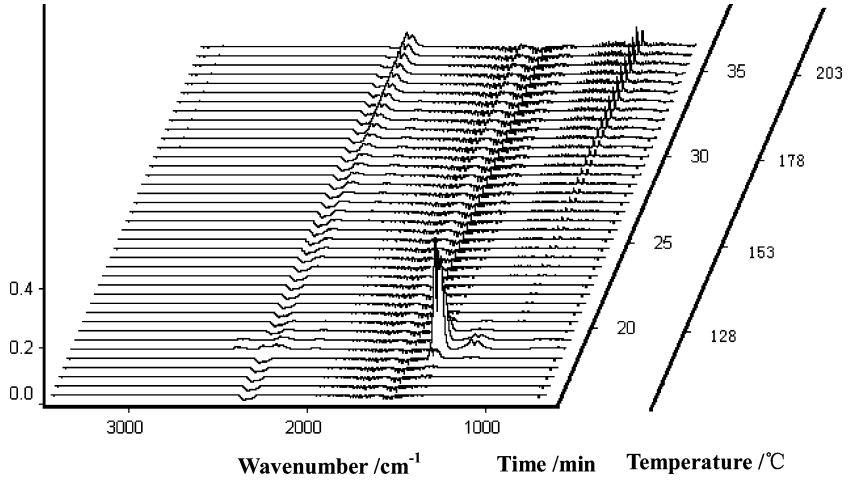

Figure 5. Online FT-IR spectra of the off-gases from the thermal decomposition of thiourea dioxide.

$$2SC(NH_2)_2(m) + HNCS(g) \rightarrow H_2N{-}CS{-}NH{-}CS{-}NH_2(m) \quad (R4)$$

$$H_2N-CS-NH-CS-NH_2\,(m) + HNCS\,(g) \rightarrow NH_3(g) + \text{(trithiocyanuric acid, s)} \quad (R5)$$

$$3HNCS(g) \rightarrow \text{(trithiocyanuric acid, s)} \quad (R6)$$

The formation of trithiocyanuric solid reduces the concentration of HNCS in the off-gases temporarily. At a higher temperature, however, trithiocyanuric solid decomposes to regenerate HNCS via the reverse process of R6. Such a decomposition is believed to be responsible for the 4.6% weight loss that occurred at the temperature above 246.2 °C (see Figure 1. TG/DSC curves). Coincidentally, the production of HNCS also reaches the peak value within the same temperature frame.

Figure 4 presents the TG/DTG/DSC curves of thiourea dioxide measured at a heating rate of 5.0 °C min^{-1}. The corresponding FT-IR spectra of the off-gases are shown in Figure 5. As is illustrated by the DSC curve, the thermal decomposition of AIMSA consists of two stages in which the first stage starts at 115.0 °C and ends at 129.0 °C and the maximum decomposition rate is reached at 118.0 °C. A significant mass loss of 17% takes place during the first stage. The IR spectra in Figure 5 indicate that a major product is SO_2(g), which has characteristic absorption peaks at 2503, 1376, 1355, 1339, 1161, and 1127 cm^{-1}.[38] Reaction R7, is suggested to account for the production of SO_2 from AIMSA.

$$NH_2(NH)CSO_2H(s) \rightarrow CO(NH_2)_2(s) + 0.5\,S(s) + 0.5\,SO_2(g) \quad (R7)$$

The above hypothesis is supported by the excellent agreements between the experimentally measured enthalpy and the theoretical value calculated from R7. The decomposition enthalpy of thiourea dioxide derived from the DSC curve equals −50.67 kJ·mol^{-1}, whereas the one calculated from reaction R7 by using formation enthalpies from literature is −50.01 kJ·mol^{-1}.[41] According to reaction R7, the expected mass loss occurred during the first stage shall be about 20.3%, which is slightly higher than the 17% detected in our experiments. Such a discrepancy may arise from two sources: (1) the impurity of the sample, which consequently makes the denominator larger than its actual value. The existence of impurity in thiourea

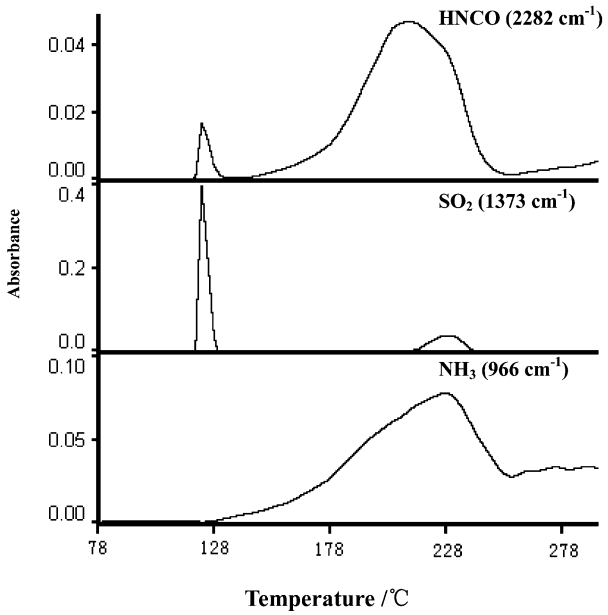

Figure 6. Absorbance vs temperature curves of three major products from the thermal decomposition of thiourea dioxide.

dioxide is supported by the detection of trace amounts of NH_3(g) (with peaks at 3331, 966, and 925 cm^{-1}) and HNCS(g) (withpeaks at 2066 and 2040 cm^{-1}), which presumably result from the decomposition of thiourea. The second source is that part of SO_2(g) is transformed into ammonium sulfite ($(NH_4)_2SO_3$(s)) which decomposes later at a higher temperature to regenerate SO_2(g) (see Figure 6). It is interesting to note that a small amount of HNCO was also detected during the first stage, although the temperature was well below both the melting (133.0 °C) and decomposition temperature (152.0 °C) of urea. The fact that HNCO and SO_2 are produced simultaneously implicates that the heat released by the exothermic reaction (R7) may have initiated local decompositions of urea.

The second stage of thiourea dioxide decomposition is governed by continuous melting, vaporization, and decomposition of urea produced from the first stage. FT-IR spectra of the evolved gases illustrate that between 129.0 and 142.0 °C there is a small amount of NH_3, but no HNCO(g) and SO_2(g). As is indicated by the fast production of large amounts of HNCO(g) and NH_3(g), the decomposition of urea increases rapidly between 142.0 and 152.0 °C, and concentrations of HNCO(g) and NH_3(g) eventually culminate, respectively, at 212.0 and 228.0 °C (see Figure 6). Thermal decompositions of urea had been

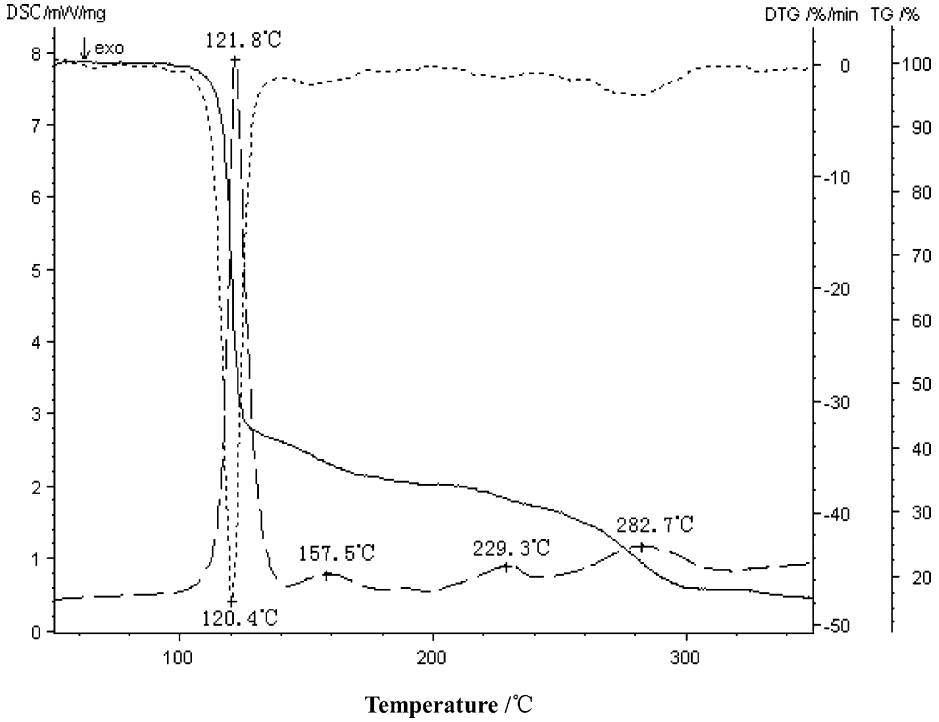

Figure 7. Simultaneous TG/DTG/DSC curves of the thermal decomposition of thiourea trioxide. The flow of nitrogen is 30.0 mL min^{-1}. The heating rate equals 8.0 °C min^{-1}, and the initial mass of thiourea trioxide is 5.30 mg.

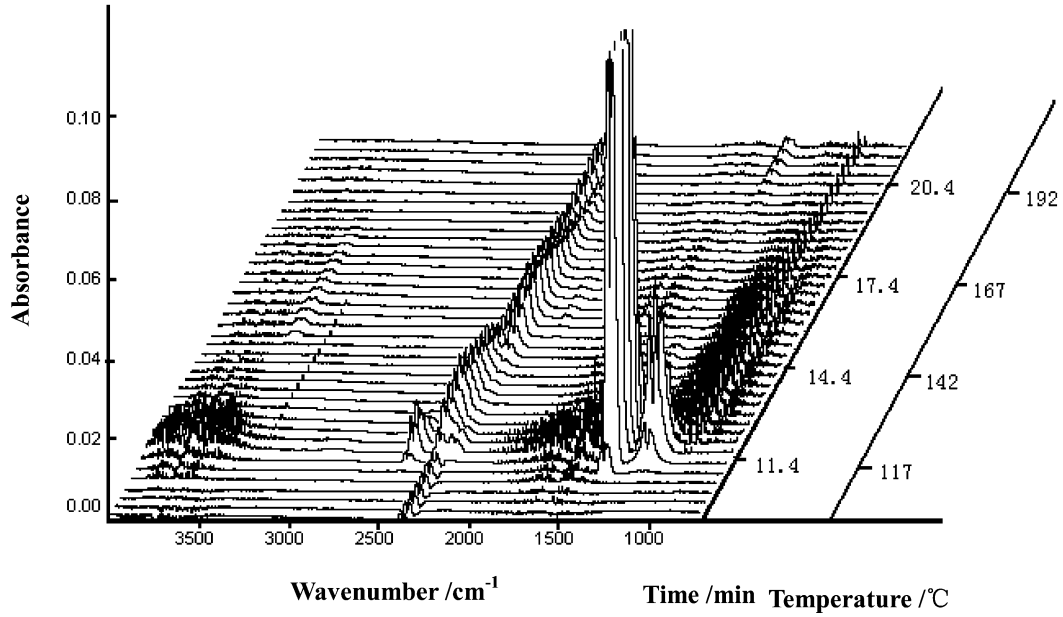

Figure 8. Online FT-IR spectra of the thiourea trioxide pyrolysis reaction. The reaction conditions are provided in Figure 7.

investigated earlier,[39] which suggests that HNCO starts to react with urea to produce biuret at approximately 160.0 °C, with biuret to form cyanuric acid (CYA: 2,4,6-trihydroxy-1,3,5-triazine), or with urea to form ammelide at about 175.0 °C, and with remaining urea to produce ammeline at 250.0 °C. However, another main product of urea decomposition, NH_3(g), reacts with CYA to go through successive nitrogen transfer to form ammelide, ammeline, and finally melamine.

Figure 7 presents the TG/DTG/DSC curves of thiourea trioxide measured at a heating rate of 8.0 °C min^{-1}. The DSC curve shows that there is one strong endothermic process, followed by three smaller ones. Such a decomposition behavior is significantly different from that of thiourea and thiourea dioxide. The real time FT-IR spectra shown in Figures 8 and 9 illustrate that SO_2(g) is detected as soon as the temperature is increased to above 107.0 °C, implicating that the first endothermic process (between 107.0 and 140.0 °C) corresponds to the formation of urea from thiourea trioxide (see reaction R8). The three small endothermic processes with peak temperatures at 157.5, 229.3, and 282.7 °C result from the continuous melting, vaporization, and decomposition of urea. As is shown in Figure 8, shortly after the appearance of SO_2(g), other products such as HNCO(g) (with absorption peaks at 2282 and 2251 cm^{-1}), NH_3(g) (peaks at 3331, 966, and 925 cm^{-1}), CO_2(g) (peaks at 2347 and 2361 cm^{-1}), and H_2O(g) (with disordered absorption bands in 3500−4000cm^{-1} and 1100−2000cm^{-1}) are detected. Similar to the decomposition of thiourea dioxide, here the

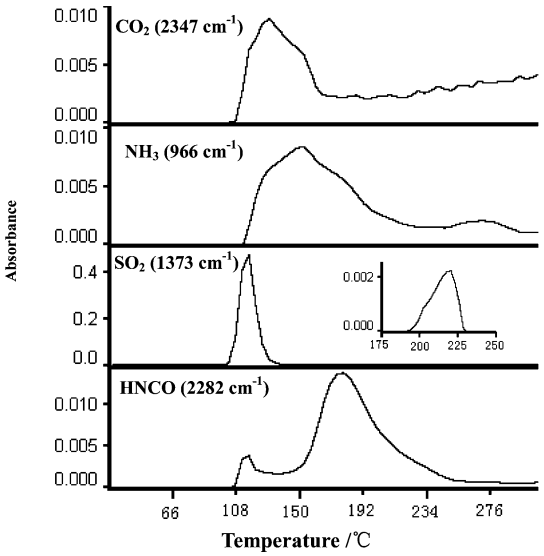

Figure 9. Absorbance vs temperature curves of four major products during the thermal decomposition of thiourea trioxide. The reaction conditions are listed in Figure 7.

TABLE 1: Peak Temperatures (T_p) of the Decomposition of Thiourea, Thiourea Dioxide, and Thiourea Trioxide under at Different Heating Rates[a]

	T_p/°C		
β/°C min^{-1}	thiourea[a]	thiourea dioxide	thiourea trioxide
2	196.1	111.9	109.0
5	214.0	118.5	117.6
8	222.1	123.7	121.8
12	234.4	127.6	126.6
15	238.1	129.2	128.6

[a] T_p corresponds to the maximum temperature of the second endothermic peak on the DSC curve.

concentration of HNCO also goes through two extremes as the reaction temperature is increased.

$$NH_2(NH)SO_3H(s) \rightarrow CO(NH_2)_2(s) + SO_2(g) \quad (R8)$$

4. Decomposition Kinetics

The Kissinger method has been used frequently in literature to determine the activation energy of solid-state reactions.[42] Expressed in the natural logarithm form, the Kissinger equation reads

$$\ln\left(\frac{\beta}{T_p^2}\right) = \ln\left(\frac{AR}{E}\right) - \frac{E}{RT_p} \quad (1)$$

where T_p is the peak temperature in the DSC curve, A is the preexponential factor, R is the gas constant, E is the apparent activation energy, and β is the heating rate, which is expressed as $\beta = dT/dt$. The activation energy, E, and the preexponential factor, A, can be obtained by plotting $\ln(\beta/(T_p)^2)$ as a function of $1/T_p$. Table 1 lists the peak temperature, T_p, of the decomposition of thiourea, thiourea dioxide, and thiourea trioxide measured at different heating rates, β. Note that the T_p values for thiourea correspond to the second endothermic peak in the thiourea DSC curve shown in Figure 1. From the plots of $\ln(\beta/(T_p)^2)$ versus $(1/T_p)$, one obtains that the activation energy, E, equals 86.30 kJ·mol^{-1} for thiourea, 138.97 kJ·mol^{-1} for thiourea dioxide, and 124.00 kJ·mol^{-1} for thiourea trioxide. The above results indicate that thiourea dioxide has the largest activation energy and preexponential factor. When Ozawa's method (eq 2),[43] which represents one of the integral methods that can determine the activation energy without knowing the reaction kinetic function, is employed to calculate E, values of 89.80 kJ·mol^{-1} for thiourea, 138.35 kJ·mol^{-1} for thiourea dioxide, and 124.08 kJ·mol^{-1} for thiourea trioxide are obtained. These calculations illustrate that both methods agree with each other very well in estimating the activation energy of the thermal decomposition of thiourea and thiourea oxides.

$$\lg \beta + \frac{0.4567\,E}{RT} = C \quad (2)$$

To establish the most probable kinetic functions for the decomposition of thiourea and thiourea oxides, the data of α (conversion ratio, $\alpha = \Delta W/\Delta W_\infty$ or $\alpha = H_t/H_0$), $d\alpha/dt$ (the rate of conversion), and T (absolute temperature) have been calculated from either the TG/DTG curve or the DSC/DDSC curves. These data are presented in Tables 2 (thiourea), 3 (thiourea dioxide), and 4 (thiourea dioxide). The values of E and A

TABLE 2: Basic Data for Thiourea Decomposition Determined by TG and DTG Curves[a]

no.	T (K)	a	$da/dT \times 10^3$ (K^{-1})	no.	T (K)	a	$da/dT \times 10^3$ (K^{-1})
1	478.15	0.2445	2.2190	11	488.15	0.5229	3.1961
2	479.15	0.2681	2.3213	12	489.15	0.5551	3.2616
3	480.15	0.2915	2.4066	13	490.15	0.5875	3.3148
4	481.15	0.3171	2.5129	14	491.15	0.6207	3.3757
5	482.15	0.3438	2.6394	15	492.15	0.6544	3.4265
6	483.15	0.3714	2.7396	16	493.15	0.6873	3.4437
7	484.15	0.3989	2.8054	17	494.15	0.7218	3.4370
8	485.15	0.4284	2.8902	18	495.15	0.7550	3.4060
9	486.15	0.4597	3.0066	19	496.15	0.7874	3.3386
10	487.15	0.4911	3.1124	20	497.15	0.8200	3.2154

[a] The heating rate, β, equals 8 °C min^{-1}. Note: $\alpha = \Delta W/\Delta W_\infty$, where ΔW is the mass loss at a certain temperature and ΔW_∞ is the maximal mass loss.

TABLE 3: Basic Data for Thiourea Dioxide Decomposition[a]

no.	T (K)	a	$da/dT \times 10^2$ (K^{-1})	no.	T (K)	a	$da/dT \times 10^2$ (K^{-1})
1	386.15	0.0405	0.2489	7	392.15	0.2444	23.9043
2	387.15	0.0460	0.4492	8	393.15	0.4028	18.7588
3	388.15	0.0538	0.8070	9	394.15	0.5758	13.5398
4	389.15	0.0662	1.5676	10	395.15	0.6558	8.9559
5	390.15	0.0799	3.3058	11	396.15	0.7598	5.3073
6	391.15	0.1561	23.1915	12	397.15	0.8180	2.8598

[a] The heating rating,β, equals 5 °C min^{-1}. Note: $\alpha = H_t/H_0$, is determined by DSC and DDSC curves, where H_t is the reaction heat at a certain time (i.e., the partial area under the DSC curve), and H_0 of -4638.99 mJ is the total heat variation (i.e., the global area under the DSC curve).

TABLE 4: Basic Data for Thiourea Trioxide Decomposition[a]

no.	T (K)	a	$da/dT \times 10^2$ (K^{-1})	no.	T (K)	a	$da/dT \times 10^2$ (K^{-1})
1	384.15	0.0194	1.2751	8	391.15	0.1383	5.4067
2	385.15	0.0250	1.4192	9	392.15	0.1930	7.3323
3	386.15	0.0323	1.6348	10	393.15	0.2680	9.4605
4	387.15	0.0420	1.9269	11	394.15	0.3614	10.9052
5	388.15	0.0551	2.3611	12	395.15	0.4642	11.0052
6	389.15	0.0735	3.0087	13	396.15	0.5649	10.0785
7	390.15	0.1000	3.9660	14	397.15	0.6552	8.7163

[a] The heating rate,β, equals 8 °C min^{-1} here. Note: $\alpha = H_t/H_0$, is determined through DSC and DDSC curves, where H_t is the reaction heat at a certain time (i.e., the partial area under the DSC curve), and H_0 of 1978.87 mJ is the total heat variation (i.e., the global area under the DSC curve).

TABLE 5: Kinetic Parameters of the Thermal Decomposition of Thiourea[a]

no.	$f(a)$	E/kJ·mol^{-1}	lg(A/s^{-1})	r	Q	d
1	$2(1-\alpha)[-\ln(1-\alpha)]^{0.5}$	88.19	7.27	0.9999	4.38×10^{-5}	3.47×10^{-9}
2	$2(1-\alpha)[-\ln(1-\alpha)]^{0.5}$	84.63	6.75	0.9999	2.34×10^{-4}	2.24×10^{-8}
3	$2(1-\alpha)[-\ln(1-\alpha)]^{0.5}$	84.87	6.81	0.9999	2.34×10^{-4}	2.22×10^{-8}
4	$2(1-\alpha)[-\ln(1-\alpha)]^{0.5}$	85.06	6.84	0.9999	2.33×10^{-4}	2.22×10^{-8}
5	$2(1-\alpha)[-\ln(1-\alpha)]^{0.5}$	92.22	6.73	0.9840	4.74×10^{-2}	7.57×10^{-4}
		mean: $E = 86.99$ kJ·mol^{-1}, lg(A/s^{-1}) = 6.88				

[a] Note: 1, Satava−Sestak method; 2, Coats−Redfern method; 3, Madhusudanan−Krishnan−Ninan method; 4, the general integral method; 5, Achar−Brindley−Sharp−Wendworth method.

TABLE 6: Kinetic Parameters of the Thermal Decomposition of Thiourea Dioxide[a]

no.	$f(a)$	E/kJ·mol^{-1}	lg(A/s^{-1})	r	$Q\times10^2$	$d\times10^3$
1	$3.4286(1-\alpha)[-\ln(1-\alpha)]^{0.7083}$	137.08	16.07	0.9842	1.1172	0.1767
2	$3.4286(1-\alpha)[-\ln(1-\alpha)]^{0.7083}$	137.64	16.13	0.9827	5.9190	1.0240
3	$3.4286(1-\alpha)[-\ln(1-\alpha)]^{0.7083}$	137.77	16.17	0.9828	5.9191	1.0203
4	$3.4286(1-\alpha)[-\ln(1-\alpha)]^{0.7083}$	137.81	16.17	0.9827	5.9192	1.0217
5	$3.4286(1-\alpha)[-\ln(1-\alpha)]^{0.7083}$	144.25	17.03	0.9847	5.7410	0.8800
		mean: $E = 138.91$ kJ·mol^{-1}, lg(A/s^{-1}) = 16.31				

[a] Note: 1, Satava−Sestak method; 2, Coats−Redfern method; 3, Madhusudanan−Krishnan−Ninan method; 4, the general integral method; 5, Broido method.

through different differential and integral methods should be approximately the same in order to ensure that the derived kinetic equation is valid; especially, they should be close to that calculated with the Ozawa and the Kissinger methods.

In this study, the following integral and differential equations have been employed to determine the most probable kinetic equations and values of E and A.

Satava−Sestak equation[44]

$$\lg[G(\alpha)] = \lg\left(\frac{AE}{\beta R}\right) - 2.315 - 0.4567\frac{E}{RT} \tag{3}$$

The general integral equation

$$\ln\left[\frac{G(\alpha)}{T^2\left(1-\frac{2RT}{E}\right)}\right] = \ln\left(\frac{AR}{\beta E}\right) - \frac{E}{RT} \tag{4}$$

Madhusudanan−Krishnan−Ninan equation[45]

$$\ln[G(\alpha)] = \left[\ln\left(\frac{AR}{\beta E}\right) + 3.772050 - 1.921503\ln E\right] - 0.120394\left(\frac{E}{RT}\right) \tag{5}$$

Coats−Redfern equation[46]

$$\ln\left[\frac{G(\alpha)}{T^2}\right] = \ln\left(\frac{AR}{\beta E}\right) - \left(\frac{E}{RT}\right) \tag{6}$$

Achar−Brindley−Sharp−Wendworth equation[47]

$$\ln\left[\frac{d\alpha/dt}{f(\alpha)}\right] = \ln A - \frac{E}{RT} \tag{7}$$

Broido equation[48]

$$\ln[G(\alpha)] = \ln\left[\frac{ART_p^2}{\beta E e^{2E/RT_p}}\right] + \frac{E}{RT_p^2}T \tag{8}$$

$f(\alpha)$ and $G(\alpha)$ in eqs 3−8 represent, respectively, the differential and integral kinetic functions. Parameters α, $d\alpha/dt$, T, T_p, A, R, E, and β are the same as defined earlier.

The calculated kinetic functions and values of E, A, r (linear correlation coefficient), Q (standard mean square deviation), and the believable factor, d, ($d = Q(1-r)$) for the decompositions of thiourea, AIMSA, and AIMSOA are listed, respectively, in Tables 5, 6, and 7. In Table 5, the calculated probable kinetic functions are $f(\alpha) = 2(1-\alpha)[-\ln(1-\alpha)]^{0.5}$, $G(\alpha) = [-\ln(1-\alpha)]^{0.5}$. Substituting $f(\alpha)$, E (86.99 kJ·mol^{-1}), and A ($10^{6.88}$) into the equation $d\alpha/dt = Af(\alpha)\exp(-E/RT)$, we obtain the kinetic equation for the thermal decomposition of thiourea as $d\alpha/dt = 2\times10^{6.88}\times\exp((-86.99\times10^3)/RT)(1-\alpha)[-\ln(1-\alpha)]^{0.5}$.

Table 6 displays the possible kinetics of the first endothermic process of AIMSA, $f(\alpha) = 3.4286(1-\alpha)[-\ln(1-\alpha)]^{0.7083}$, $G(\alpha) = [-\ln(1-\alpha)]^{0.2917}$. The kinetic equation of this process should be stated as $d\alpha/dt = 3.4286\times10^{16.31}\times\exp((-138.91\times10^3)/RT)(1-\alpha)[-\ln(1-\alpha)]^{0.7083}$. As for the first exothermic process of AIMSOA, the most probable kinetic function is $3(1-\alpha)[-\ln(1-\alpha)]^{2/3}$ and $G(\alpha) = [-\ln(1-\alpha)]^{1/3}$; the kinetic equation is $d\alpha/dt = 2\times10^{15.22}\times\exp((-129.44\times10^3)/RT)(1-\alpha)[-\ln(1-\alpha)]^{2/3}$. Notably, the kinetic functions of thiourea, thiourea dioxide, and thiourea trioxide all assemble the Johnson−Mehl−Avrami Equation $f(\alpha) = n(1-\alpha)-[-\ln(1-\alpha)^{1-1/n}$ and $G(\alpha) = [-\ln(1-\alpha)]^{1/n.}$, with $n = 2$, 3.43, and 3, respectively. Such a result implicates that the transformation of thiourea, AIMSA, and AIMSOA features random and continuous nucleation. Remarkably, the linear correlation coefficients (r) of those calculations are all above 0.98, whereas their standard mean square deviations (Q) are all below 0.3.

The entropy ($\Delta S^{\ddagger}$), enthalpy ($\Delta H^{\ddagger}$), and Gibbs energy ($\Delta G^{\ddagger}$) of the thermal decomposition of thiourea, AIMSA, and AIMSOA are calculated with eqs 9−11, and these values are summarized in Table 8. The temperatures used in these calculations equal T_{p0}, which correspond to the peak temperature, T_p, at the heating rate $\beta \to 0$. Calculated through the equation $T_{pi} = T_{p0} + b\beta_i + c\beta_i^2 + d\beta_i^3$, where $i = 1$, 2, 3, 4, and 5 and b, c, and d are coefficients, the values of T_{p0} for thiourea,

TABLE 7: Kinetic Parameters of the Thermal Decomposition of Thiourea Trioxide[a]

no.	$f(a)$	E/kJ·mol^{-1}	lg(A/s^{-1})	r	$Q \times 10^2$	$d \times 10^5$
1	$3(1-\alpha)[-\ln(1-\alpha)]^{2/3}$	128.33	15.01	0.9980	0.1918	0.3778
2	$3(1-\alpha)[-\ln(1-\alpha)]^{2/3}$	128.46	15.02	0.9978	1.0118	2.1868
3	$3(1-\alpha)[-\ln(1-\alpha)]^{2/3}$	128.59	15.06	0.9978	1.0120	2.1791
4	$3(1-\alpha)[-\ln(1-\alpha)]^{2/3}$	128.63	15.02	0.9978	1.0118	2.1868
5	$3(1-\alpha)[-\ln(1-\alpha)]^{2/3}$	133.20	16.01	0.9984	0.8134	1.2806
	mean: $E = 129.44$ kJ·mol^{-1}, lg(A/s^{-1}) = 15.22					

[a] Note: 1, Satava−Sestak method; 2, Coats−Redfern method; 3, Madhusudanan−Krishnan−Ninan method; 4, the general integral method; 5, Broido method.

TABLE 8: The Entropy, Enthalpy, and Free Energy of Activation for Thiourea and Its Oxides

species	T_{po}/K	$\Delta S^{\ddagger}$/JK^{-1} mol^{-1}	$\Delta H^{\ddagger}$/kJ·mol^{-1}	$\Delta G^{\ddagger}$/kJ·mol^{-1}
thiourea	455.36	−118.06	86.30	140.06
thiourea dioxide	379.43	68.00	138.97	113.17
thiourea trioxide	374.63	64.47	124.00	99.85

AIMSA, and AIMSOA are 455.36, 379.43, and 374.63 K, respectively.

$$A = \frac{k_B T}{h} \exp^{\Delta S^{\ddagger}/R} \tag{9}$$

$$A \exp(-E/RT) = \frac{k_B T}{h} \exp\left(\frac{\Delta S^{\ddagger}}{R}\right) \exp\left(\frac{-\Delta H^{\ddagger}}{RT}\right) \tag{10}$$

$$\Delta G^{\ddagger} = \Delta H^{\ddagger} - T\Delta S^{\ddagger} \tag{11}$$

where k_B is the Boltzmann constant and h is the Planck's constant. These thermodynamic parameters, especially the data of $\Delta G^{\ddagger}$, illustrate that the thermal stability of thiourea and its oxides is in the order of TU ≫ AIMSA > AIMSOA.

5. Conclusions

Complementing earlier studies on oxidation of thiourea,[21−29] thermal decomposition reactions of thiourea and thiourea oxides (AIMSA and AIMSOA) are investigated in this study by a simultaneous TG/DTG/DSC/FT-IR method in nitrogen atmosphere. The decomposition of thiourea is found to go through two stages, that is, the isomerization of thiourea and its subsequent thermal decomposition. Three major products, for example, carbon disulfide (CS_2(g)), isothiocyanic acid (HNCS(g)), and ammonia (NH_3(g)), have been identified by the online FT-IR spectra. Theoretical calculations show that the endothermic decomposition of thiourea is characterized by the kinetics $d\alpha/dt = 2 \times 10^{6.88} \times \exp((-86.99 \times 10^3)/RT)(1-\alpha)[-\ln(1-\alpha)]^{0.5}$, where α represents the relative weight loss.

Thermal decompositions of thiourea dioxide, however, commence with a strongly exothermic process, leading to the production of urea(s) and sulfur dioxide SO_2(g). The heat released by the decomposition of AIMSA appears to initialize local decompositions of urea, as evidenced by the production of NH_3 at the temperature that is even below the melting temperature of urea. Kinetic analysis of the decomposition of thiourea dioxide results in the following rate law, $d\alpha/dt = 3.4286 \times 10^{16.31} \times \exp((-138.91 \times 10^3)/RT)(1-\alpha)[-\ln(1-\alpha)]^{0.7083}$. Following the first stage, urea decomposes at a higher temperature, where three products, HNCO, NH_3, and SO_2 are detected in the off-gases. As opposed to the exothermic decomposition of thiourea dioxide, the decomposition of thiourea trioxide is strongly endothermic, leading to the production of urea(s) and SO_2(g). The kinetics of such an endothermic decomposition is found to be $d\alpha/dt = 2 \times 10^{15.22} \times \exp((-129.44 \times 10^3)/RT)(1-\alpha)[-\ln(1-\alpha)]^{2/3}$. Subsequent decompositions of urea lead to productions of HNCO(g), NH_3(g), CO_2(g), and H_2O(g).

In summary, although the decomposition of thiourea and thiourea oxides appears to evolve differently, their decomposition kinetics follow the Johnson−Mehl−Avrami equation $f(\alpha) = n(1-\alpha)-[-\ln(1-\alpha)^{1-1/n}$ and $G(\alpha) = [-\ln(1-\alpha)]^{1/n.}$ with $n = 2$, 3.43, and 3, respectively. This implicates that the decomposition of thiourea and its oxides features random and continuous nucleation during the transformation process. Calculations of the Gibbs energy of activation ($\Delta G^{\ddagger}$) illustrate that thiourea is thermodynamically more stable than its oxides. The online FT-IR analysis illustrates that productions of different species reach the maximum at different temperatures. This information is important in selectively manipulating the decomposition products of thiourea and thiourea oxides for the benefit of industrial production, environmental protection, and so forth.

Acknowledgment. This work is supported through NSFC (20103010, 20471043), EYTP of China, and Zhejiang Provincial Natural Science Foundation of China (Y404118). J.W. is sponsored by NSERC.

References and Notes

(1) Vázquez, L.; Salvarezza, R. C.; Arvia, A. J. *Phys. Rev. Lett.* **1997**, *79*, 709−712.
(2) González, S.; Laz, M. M.; Souto, R. M.; Salvarezza, R. C.; Arvia, A. J. *Corrosion* **1993**, *49*, 450−546.
(3) Jagodziński, T. S. *Chem. Rev.* **2003**, *103*, 197−227.
(4) Ayres, J. A. *Decontamination of Nuclear Reactors and Equipment*; Ronald Press Co.: New York, 1970; p 177.
(5) Arifoglu, M.; Marmer, W. N.; Dudley, R. R. *Tex. Res. J.* **1992**, *62*, 94−100.
(6) El-Rafie, M. H.; Zahran, M. K.; El-Tahlawy, Kh. F.; Hebeish, A. *Polym. Degrad. Stab.* **1995**, *47*, 73−85.
(7) Abdel-Hafiz, S. A. *J. Appl. Polym. Sci.* **1995**, *58*, 2005−2011.
(8) Miller, A. E.; Bischoff, J. J.; Pae, K. *Chem. Res. Toxicol.* **1988**, *1*, 169−174.
(9) Maryanoff, R. C.; Stanzione, R. C.; Plampin, J. N.; Mills, J. E. *J. Org. Chem.* **1986**, *51*, 1882−1884.
(10) Kim, K.; Lin, Y.-T.; Mosher, H. S. *Tetrahedron Lett.* **1988**, *29*, 3183−3186.
(11) Olah, G. A.; Burrichter, A.; Rasul, G.; Hachoumy, M.; Prakash, G. K. S. *J. Am. Chem. Soc.* **1997**, *119*, 12929−12933.
(12) Whitesides, G. M.; Ismagilov, R. F. *Science* **1999**, *284*, 89−92.
(13) Epstein, I. R.; Pojman, J. A. *An Introduction to Nonlinear Chemical Dynamics: Oscillations, Waves, Patterns and Chaos*; Oxford University Press: New York, 1998.
(14) *Oscillations and Traveling Waves in Chemical Systems*; Field, R. J., Burger, M., Eds.; Wiley-Interscience: New York, 1985.
(15) *Chemical Waves and Patterns*; Kapral, R., Showalter, K., Eds.; Kluwer Academic Publishers: Dordrecht, The Netherlands, 1995.
(16) Scott, S. K. *Chemical Chaos*; Oxford University Press: Oxford, U.K., 1991.
(17) Rabai, G.; Beck, M. T. *J. Chem. Soc., Dalton Trans.* **1985**, 1669−1672.
(18) Simoyi, R. H.; Epstein, I. R. *J. Phys. Chem.* **1987**, *91*, 5124−5128.

(19) Doona, C. J.; Blittersdorf, R.; Schneider, F. W. *J. Phys. Chem.* **1993**, *97*, 7258−7263.
(20) Gao, Q.-Y.; Wang, J.-C. *Chem. Phys. Lett.* **2004**, *391*, 349−353.
(21) Chinake, C. R.; Simoyi, R. H. *J. Phys. Chem.* **1994**, *98*, 4012−4019.
(22) Chikwana, E.; Otoikhian, A.; Simoyi, R. H. *J. Phys. Chem. A* **2004**, *108*, 11591−11599.
(23) Epstein, I. R.; Kustin, K.; Simoyi, R. H. *J. Phys. Chem.* **1992**, *96*, 5852−5856.
(24) Chigwana, T. R.; Simoyi, R. H. *J. Phys. Chem. A* **2005**, *109*, 1094−1104.
(25) Rábai, G.; Wang, R. T.; Kustin, K. *Int. J. Chem. Kinet.* **1993**, *25*, 53−62.
(26) Sharma, V. K.; Rivera, W.; Joshi, V. N.; Millero, F. J.; O'Connor, D. *Environ. Sci. Technol.* **1999**, *33*, 2645−2650.
(27) Wang, W.-F.; Schuchmann, M. N.; Schuchmann, H.-P.; Knolle, W.; von Sonntag, J.; von Sonntag, C. *J. Am. Chem. Soc.* **1999**, *121*, 238−245.
(28) Olojo, R.; Simoyi, R. H. *J. Phys. Chem. A* **2004**, *108*, 1018−1023.
(29) Rabai, G.; Orban, M. *J. Phys. Chem.* **1993**, *97*, 5935−5939.
(30) Rushing, C. W.; Thompson, R. C.; Gao, Q.-Y. *J. Phys. Chem. A* **2000**, *104*, 11561−11565.
(31) Xu, L. -Q.; Gao, Q.-Y.; Feng, J.-M.; Wang, J.-C. *Chem. Phys. Lett.* **2004**, *397*, 265−270.
(32) Svarovsky, S. A.; Simoyi, R. H.; Makarov, S. V. *J. Phys. Chem. B* **2001**, *105*, 12634−12643.
(33) Vesilind, P. A.; Peirce, J. J. *Environmental Pollution and Control*, 2nd ed.; Butterworth: Boston, MA, 1983.
(34) Miller, A. E. *Synthesis* **1986**, *9*, 777−779.
(35) Stradella, L.; Argentero, M. *Thermochem. Acta* **1993**, 315−323.
(36) Kim, K.-J.; Lee, C.-H.; Ryu, S.-k. *J. Chem. Eng. Data* **1994**, *39*, 228−230.
(37) Donnelly, J. R.; Drewes, L. A.; Johnson, R. L.; Munslow, W. D.; Knapp, K. K.; Sovocool, G. W. *Thermochim. Acta* **1990**, *167*, 155−187.
(38) Madarász, J.; Bombicz, P.; Okuya, M.; Kaneko, S.; Pokol, G. *J. Anal. Appl. Pyrolysis* **2004**, *72*, 209−214.
(39) Schaber, P. M.; Colson, J.; Higgins, S.; Thielen, D.; Anspach, Brauer, B. J. *Thermochim. Acta* **2004**, *424*, 131−142; and references therein.
(40) Ostrogovich, G.; Bacaloglu, R. *Rev. Roum. Chim.* **1965**, *10*, 1111−1123; and references therein.
(41) Chase, M. W., Jr. NIST-JANAF Themochemical Tables, 4th ed., *J. Phys. Chem. Ref. Data*, *Monograph 9* **1998**, 1−1951.
(42) Kissinger, H. E. *Anal. Chem.* **1957**, *29*, 1702−1706.
(43) Ozawa, T. A. *Bull. Chem. Soc. Jpn.* **1965**, *38*, 1881−1886.
(44) Satava, V.; Sestak, J. *J. Therm. Anal.* **1975**, *8*, 477−489.
(45) Madhusudanan, P. M.; Krishnan, K.; Ninan, K. N. *Thermochim. Acta* **1986**, *97*, 189−201.
(46) Coats, A. W.; Redfern, J. P. *Nature* **1964**, *201*, 68−69.
(47) Sharp, J. H.; Wendworth, S. A. *Anal. Chem.* **1960**, *32*, 1558−1563.
(48) Broido, A. *J. Polym. Sci., Part A-2* **1969**, *7*, 1761−1773.